Different characteristic effects of ageing on starch-based films plasticised by 1-ethyl-3-methylimidazolium acetate and by glycerol

Binjia Zhang [a,b,c], Fengwei Xie [b,d*], Tianlong Zhang, [b,e] Ling Chen [a†], Xiaoxi Li [a], Rowan W. Truss [d], Peter J. Halley [b,d], Julia L. Shamshina [f,g], Tony McNally [h], Robin D. Rogers [f,i]

[a] *Ministry of Education Engineering Research Center of Starch & Protein Processing, Guangdong Province Key Laboratory for Green Processing of Natural Products and Product Safety, College of Light Industry and Food Sciences, South China University of Technology, Guangzhou 510640, China*

[b] *Australian Institute for Bioengineering and Nanotechnology, The University of Queensland, Brisbane, Qld 4072, Australia*

[c] *College of Food Science and Technology, Huazhong Agricultural University, Wuhan 430070, China*

[d] *School of Chemical Engineering, The University of Queensland, Brisbane, Qld 4072, Australia*

[e] *School of Chemistry and Molecular Biosciences, The University of Queensland, Brisbane, Qld 4072, Australia*

[f] *The University of Alabama, Tuscaloosa, AL 35487, USA*

[g] *525 Solutions, Inc., 720 2nd Street, Tuscaloosa, AL 35401, USA*

[h] *International Institute for Nanocomposites Manufacturing (IINM), WMG, University of Warwick, CV4 7AL, UK*

[i] *Department of Chemistry, McGill University, 801 Sherbrooke St. West, Montreal, QC H3A 0B8, Canada*

[*] Corresponding author. Tel.: +61 7 3346 3199; fax: +61 7 3346 3973.

Email address: f.xie@uq.edu.au, fwhsieh@gmail.com (F. Xie).

[†] Corresponding author. Tel.: +86 20 8711 3252; fax: +86 20 8711 3252.

Email address: felchen@scut.edu.cn (L. Chen).

ABSTRACT

The focus of this study was on the effects of plasticisers (the ionic liquid 1-ethyl-3-methylimidazolium acetate, or [Emim][OAc]; and glycerol) on the changes of starch structure on multiple length scales, and the variation in properties of plasticised starch-based films, during ageing. The films were prepared by a simple melt compression moulding process, followed by storage at different relative humidity (RH) environments. Compared with glycerol, [Emim][OAc] could result in greater homogeneity in [Emim][OAc]-plasticised starch-based films (no gel-like aggregates and less molecular order (crystallites) on the nano-scale). Besides, much weaker starch-starch interactions but stronger starch-[Emim][OAc] interactions at the molecular level led to reduced strength and stiffness but increased flexibility of the films. More importantly, [Emim][OAc] (especially at high content) was revealed to more effectively maintain the plasticised state during ageing than glycerol: the densification (especially in the amorphous regions) was suppressed; and the structural characteristics especially on the nano-scale were stabilised (especially at a high RH), presumably due to the suppressed starch molecular interactions by [Emim][OAc] as confirmed by Raman spectroscopy. Such behaviour contributed to stabilised mechanical properties. Nonetheless, the crystallinity and thermal stability of starch-based films with both plasticisers were much less affected by ageing and moisture uptake during storage (42 days), but mostly depended on the plasticiser type and content. As starch is a typical semi-crystalline bio-polymer containing abundant hydroxyl groups and strong hydrogen bonding, the findings here could also be significant in creating materials from other similar biopolymers with tailored sensitivity and properties to the environment.

Keywords:

Starch-based materials; Ionic liquid; 1-Ethyl-3-methylimidazolium acetate; Plasticizer; Relative Humidity; Ageing

Chemical compounds studied in this article

Starch (PubChem CID: 24836924); Water (PubChem CID: 962); Glycerol (PubChem CID: 753); 1-Ethyl-3-methylimidazolium acetate (PubChem CID: 11658353)

1. Introduction

Currently, biomaterials are increasingly selected for reasons of environmental sustainability and carbon impact. Biopolymers can generally be referred to as polymers derived from biomass, a natural permanent and underutilised source of renewable feedstock with the principal renewable biopolymers being cellulose, chitosan/chitin, starch, and lignin. Biopolymers are not only widely available and sustainable, but also biodegradable and biocompatible, and thus have several economic and environmental advantages. The growing interest from society in environmentally-friendly materials creates a demand for technically advantageous products that can replace petroleum-derived materials.

Among these groups of polymers, starch, a polysaccharide found in plants such as maize (corn), potato, cassava, wheat, and rice, represents a typical model with a naturally complex structure involving strong intermolecular hydrogen bonding. In a native form of granules (<1 μm~100 μm), starch has a hierarchical multi-level structure which is based on two major bio-macromolecules, amylose (mainly linear) and amylopectin (hyper-branched) (~nm); but between the granule and molecular levels, there are alternating amorphous and semicrystalline shells (growth rings) (100~400 nm), with the latter shell

being stacked crystalline and amorphous lamellae (periodicity) (9~10 nm) (Fu, Wang, Li, Wei, & Adhikari, 2011; Jane, 2009; Pérez, Baldwin, & Gallant, 2009; Pérez & Bertoft, 2010). Therefore, it is important to understand the complex structure of starch and how it can be altered to achieve desired forms (*e.g.*, a plasticised form).

With a plasticiser and elevated temperature, a process known as "gelatinisation" (with abundant plasticiser content) or "melting" (with limited plasticiser content) occurs, resulting in disruption of the 3D structure of native starch; and, if preferential conditions are reached, this can lead to a homogeneous amorphous material known as "thermoplastic starch (TPS)" or "plasticised starch", which is essential in the production of some starch-based materials (Avérous, 2004; Liu, Xie, Yu, Chen, & Li, 2009a; Xie, Halley, & Avérous, 2012; Xie, Pollet, Halley, & Avérous, 2013). While water is the most commonly-used plasticiser for starch, substances such as polyols (glycerol, glycol, sorbitol, etc.), compounds containing nitrogen (urea, ammonium derived, amines), and citric acid have also been reported to be effective in the plasticisation of starch (Liu et al., 2009a; Xie et al., 2012). A plasticiser for starch should preferably be stable (non-volatile) both during thermal processing and in post-processing stages, be ineffective in starch macromolecular degradation, be safe to humans and the environment, and be able to provide starch-based materials with enhanced performance and new capabilities. Unfortunately, commonly-used plasticisers do not yet have all the desired attributes and thus finding alternative and better plasticisers for starch is of interest.

Ionic liquids (IL, salts with melting points below 100 °C) that consist of an imidazolium (less often pyridinium, ammonium, or phosphonium) cation and a strongly basic, hydrogen bond accepting anion (*e.g.*, carboxylates or halides) have the ability to fully or partially disrupt the intermolecular hydrogen bonding present in biopolymeric networks, and as a result, either fully dissolve or plasticise many biopolymers such as starch (Biswas, Shogren, Stevenson, Willett, & Bhowmik, 2006; El Seoud,

Koschella, Fidale, Dorn, & Heinze, 2007; Wilpiszewska & Spychaj, 2011; Zakrzewska, Bogel-Łukasik, & Bogel-Łukasik, 2010; Zhu et al., 2006), cellulose (Heinze, Schwikal, & Barthel, 2005; Zhang, Wu, Zhang, & He, 2005), chitin/chitosan (Qin, Lu, Sun, & Rogers, 2010; Wu, Sasaki, Irie, & Sakurai, 2008; Xie, Zhang, & Li, 2006), silk fibroin (Phillips et al., 2004; Wang, Yang, Chen, & Shao, 2012; Wang, Chen, Yang, & Shao, 2013), lignin (Pu, Jiang, & Ragauskas, 2007), zein protein (Biswas et al., 2006), and wool keratin (Xie, Li, & Zhang, 2005). These IL's thus can be used as excellent media for polysaccharide plasticisation and modification resulting in the development of advanced biomaterials, such as ionically conducting polymers or solid polymer electrolytes (Liew, Ramesh, Ramesh, & Arof, 2012; Liew & Ramesh, 2015; Ramesh, Liew, & Arof, 2011a; Ramesh, Shanti, Morris, & Durairaj, 2011b; Ramesh, Shanti, & Morris, 2012; Wang, Zhang, Liu, & He, 2009a; Wang, Zhang, Wang, & Liu, 2009b; Wang, Zhang, Liu, & Han, 2010). It is quite well known that there is a near infinite variety of combinations of ions that will lead to salts which can be defined as IL's. So even though some IL's are somewhat toxic, there are still many IL's that can be synthesised via chemistry and considered as "green" solvents for biopolymers. For example, 1-ethyl-3-methylimidazolium acetate ([Emim][OAc]) has desirable properties, e.g., low toxicity (LD50 > 2000 $mg \cdot kg^{-1}$), low corrosiveness, low melting point (< −20 °C), low viscosity (10 mPa·s at 80 °C), and favourable biodegradability (Wang, Gurau, & Rogers, 2012).

For the processing of polysaccharides with IL's, while solution methods were predominantly involved in previous studies, melt processing should be more relevant to industrial application as much less solvent is required with higher anticipated plasticisation. Sankri et al. (2010) and Leroy, Jacquet, Coativy, Reguerre, and Lourdin (2012) have done pioneering work using an IL (1-butyl-3-methylimidazolium chloride, or [C_4mim][Cl]) as a new plasticiser for melt processing of starch-based materials, which demonstrated improved plasticisation, electrical conductivity, and hydrophobicity. Our

previous work (Xie et al., 2014) has shown that [Emim][OAc] has a significant plasticisation effect on starch, including high-amylose starch, prepared via a simple compression moulding process, and can reduce the crystallinity and make the amorphous phase more mobile, the property advantageous for some specific applications (*e.g.* electrically-conductive materials). Especially interestingly, plasticisation by [Emim][OAc] can make the effect of amylose content insignificant, contrary to most studies where other plasticisers were used showing the close relationship between the amylose content and the starch structure and properties (Xie et al., 2015).

For the development of high performance biopolymer-based materials, it is more important to understand the structural and property evolution of such materials during storage (ageing) and to explore for solutions to realise stabilised properties. This is because biopolymers such as starch, cellulose, and chitosan are generally highly hydrophilic due to their abundant hydroxyl functionality, which leads to their extremely high sensitivity to environmental moisture. There have been many studies of the ageing-induced changes of starch-based materials with traditional plasticisers (*e.g.* glycerol). Forssell, Hulleman, Myllärinen, Moates, and Parker (1999) investigated ageing of thermoplastic barley and oat starches prepared by extrusion. In their study, glycerol-plasticised thermoplastic starches were stored in the rubbery state at 20 °C and 50% relative humidity (RH) for 8 months. It was suggested that the main mechanism underlying the changes in mechanical failure properties was slow amylopectin recrystallisation. Using ^{1}H pulsed NMR and wide-angle X-ray diffraction (XRD), Farhat, Blanshard, and Mitchell (2000) discovered that the rate of retrogradation (recrystallisation) of waxy maize starch extrudates depended strongly on the water content in the sample and storage temperature. Shi et al. (2007) prepared plasticised starch-based materials with high glycerol contents (30 to 60 wt%) by melt blending. At 37 °C and 50% RH, the ageing speed was found to closely relate to the plasticiser content. When the glycerol content was high (50–60%) , it had no obvious effect on mechanical properties, as a

high content of glycerol promoted the formation of single-helical structure of V-type, but inhibited the double-helical structure of B-type. Schmitt et al. (2015) studied the evolution of structure and properties of starch-based materials formulated with different plasticisers such as polyols and urea/ethanolamine blends prepared by melt extrusion. Their results showed that urea/ethanolamine was the most effective in limiting starch retrogradation, while polyol-plasticised samples exhibited apparently increased stiffening and reduced ductility during storage (attributed to re-ordering of amylopectin as indicated by increased B-type crystallinity). Nonetheless, publications scarcely exist on the ageing of starch-based materials plasticised by IL's. Bendaoud and Chalamet (2013) reported that compared with glycerol, IL's (1-allyl-3-methylimidazolium chloride, or [Amim][Cl]; and 1-butyl-3-methylimidazolium chloride, or [C_4mim][Cl]) could result in plasticised starch with a lower affinity to water adsorption and greater depression in glass transition temperature.

Therefore, this paper reports our efforts aimed at comparing and understanding the different performance of two plasticisers, glycerol and [Emim][OAc], in maintaining the material characteristics of starch-based plastics during ageing. This research was based on our established protocol (Xie et al., 2014; Xie et al., 2015) to use a simple one-step compression moulding process to minimise the effect of shear-induced macromolecular degradation during processing. The ageing process was carried out under different fixed RH environments. As a novel approach, we studied the structural evolution over a range of length scales (molecular, lamellar and crystalline structures), and the changes in properties (mechanical properties and thermal stability), of starch-based films before and after ageing, and explored the mechanism behind the phenomena. The findings here could be significant in creating different biopolymer-based materials with tailored sensitivity and properties to the environment.

2. Materials and Methods

2.1. Materials

A high-amylose maize starch supplied by Ingredion ANZ Pty Ltd (Lane Cove, NSW, Australia), with its commercial name as "Gelose 80", was used in this work. This is a genetically-modified starch product, with its amylose content being 82.9% as measured previously (Tan, Flanagan, Halley, Whittaker, & Gidley, 2007). This starch is chemically unmodified; and its original moisture content was 14.1 wt%, as measured by a Satorius Moisture Analyser (Model MA30, Sartorius Weighing Technology GmbH, Weender Landstraβe 94–108, 37075, Goettingen, Germany). Milli-Q water was used in all instances. Glycerol (AR) was supplied by Chem-Supply Pty Ltd (Gillman, SA, Australia) and used as received. [Emim][OAc] of purity ≥95%, produced by IoLiTec Ionic Liquids Technologies GmbH (Salzstraβe 184, D-74076 Heilbronn, Germany), was also supplied by Chem-Supply Pty Ltd. [Emim][OAc] was used as received without further purification. As [Emim][OAc] was liquid at room temperature and miscible with water (Mateyawa et al., 2013), different ratios of water:[Emim][OAc] mixture could be easily prepared in vials for subsequent use.

2.2. Sample preparation

Formulations for sample preparation are shown in Table 1. In Table 1 and the following text, the plasticised starch samples are coded in the format of "S91/G9-L", where "S" denotes the starch, the number "91" shows the weight content of starch, the number "9" indicates the weight content of either ionic liquid ("E") or glycerol ("G"), and "L" means the RH during ageing (either "L", low, 33%; or "H", high, 75%). In the meantime, we use "S91/G9" to denote the sample before ageing. Based on our preliminary work (Xie et al., 2014; Xie et al., 2015), either glycerol or [Emim][OAc] was firstly mixed with water, and then the mixed solution (30 wt%) was added into the starch (wet basis, 100 wt%,

containing 14.1% moisture content). For the preparation of S91/G9 or S91/E9, the ratio of glycerol:water or [Emim][OAc]:water was 3:7 (wt/wt), whereas for S76/G24 or S76/E24 the ratio was 9:1 (wt/wt). The liquid mixture was added drop-wise to the starch, accompanied by careful blending using a mortar and pestle to ensure an even distribution of the liquid mixture in the starch. Then, the blended samples were hermetically stored in ziplock bags at 4 °C for at least overnight, before thermal compression moulding. This allowed time for further equilibration of the samples. The powder was carefully and equally spread over the moulding area with poly(tetrafluoroethylene) glass fabrics (Dotmar EPP Pty Ltd, Acacia Ridge, Qld, Australia) located between the starch and the mould, then compression moulded at 160 °C and 6 MPa for 10 min, followed by rapid cooling to room temperature (RT) before opening the mould and retrieving the sample (thickness approx. 1.2 mm). The films were conditioned at different RH's, 33% (over saturated magnesium chloride solution), and 75% (over saturated sodium chloride solution), at RT in desiccators for 42 days before any characterisation of the materials. After the conditioning, the thickness of the films was about 1 mm.

From sample preparation to ageing, no observation indicated that [Emim][OAc] phased out of the starch films which might make the films sticky. This suggest a strong binding between [Emim][OAc] and starch.

[Insert Table 1 here]

According to our preliminary work (Xie et al., 2014), the use of compression moulding under the described conditions should mostly destroy the starch granules so that plasticised starch could be formed.

2.3. Characterisation

2.3.1. Moisture uptake during ageing

The water uptake behaviour of plasticised starch-base films during ageing was monitored. After compression moulding, the films were cut into tensile testing specimens (details below in Section 2.3.2), which were dried at 50 °C under vacuum for 48 h. This drying condition could avoid glycerol volatilisation but sufficiently remove all the moisture in the films (*i.e.*, the "zero" value of moisture content). The dried samples were immediately stored in a desiccator with P_2O_5 until the samples reached room temperature (RT). Then samples were weighed, to obtain the weight values after drying, after which the samples were stored at different specific RH's (L, 33%, over saturated magnesium chloride solution; and H, 75%, over saturated sodium chloride solution) and then weighed as a function of time. Five replicates of each sample were measured. The moisture content W (%) was calculated according to Eq. (1) where M_t is the weight at time t and M_d is the weight immediately after drying.

$$W\ (\%) = \frac{M_t - M_d}{M_d} \times 100 \qquad (1)$$

2.3.2. Tensile testing

Tensile tests were performed with an Instron® 5543 universal testing machine (Instron Pty Ltd, Bayswater, Vic., Australia) with a 500N load cell on dumbbell-shaped specimens cut from the sheets with a constant deformation rate of 10 mm/min at room temperature. The specimens corresponded to Type 4 of the Australian Standard AS 1683:11 (ISO 37:1994), and the testing section of each specimen was 12 mm in length and 2 mm in width. Young's modulus (E), tensile strength (σ_t), and elongation at

224 break (ε_b) were determined by the Instron® computer software, from at least 7 specimens for each of the
225 plasticised starch samples.
226
227 *2.3.3. Thermogravimetric analysis (TGA)*
228 A Mettler Toledo TGA/DSC1 machine (Mettler-Toledo Ltd., Port Melbourne, Vic., Australia),
229 calibrated using the melting points of Au, Zn and In standards (1064 °C, 419.5 °C, and 155.6 °C,
230 respectively), was used with 40 μL aluminium crucibles with a cap with a pinhole for thermogravimetric
231 analysis (TGA) under nitrogen. A sample mass of about 5 mg was used for each run. The samples were
232 heated from 25 °C to 550 °C and measured in the dynamic heating regime, using a constant heating
233 ramp of 3 K/min.
234
235 *2.3.4. X-ray diffraction (XRD)*
236 The starch samples were placed in the sample holder of a powder X-ray diffractometer (D8 Advance,
237 Bruker AXS Inc., Madison, WI, USA) equipped with a graphite monochromator, a copper target, and a
238 scintillation counter detector. XRD patterns were recorded for an angular range (2θ) of 4–40°, with a
239 step size of 0.02° and a step rate of 0.5 s per step, and thus the scan time lasted for approximately 15 min.
240 The radiation parameters were set as 40 kV and 30 mA, with a slit of 2 mm. Traces were processed
241 using the Diffracplus Evaluation Package (Version 11.0, Bruker AXS Inc., Madison, WI, USA) to
242 determine the X-ray diffractograms of the samples. The degree of crystallinity was calculated using the
243 method of Lopez-Rubio, Flanagan, Gilbert, and Gidley (2008) with the PeakFit software (Version 4.12,
244 Systat Software, Inc., San Jose, CA, USA), Eq. (1):
245

$$X_c = \frac{\sum_{i=1}^{n} A_{ci}}{A_t} \quad (2)$$

where A_{ci} is the area under each crystalline peak with index i, and A_t is the total area (both amorphous background and crystalline peaks) under the diffractogram.

The V-type crystallinity (single-helical amylose structure) was calculated based on the total crystalline peak areas at 7.5, 13, 20, and 23° (van Soest, Hulleman, de Wit, & Vliegenthart, 1996).

2.3.5. Synchrotron small-angle X-ray scattering (SAXS)

SAXS analysis was carried out on the SAXS/WAXS beamline (flux, 10^{13} photons/s) at the Australian Synchrotron (Clayton, Vic., Australia), at a wavelength λ = 1.47 Å. The 2D scattering patterns were collected using a Pilatus 1M camera (active area 169 × 179 mm; and pixel size 172 × 172 μm). The scatterBrain software was used to acquire the one-dimensional (1D) data from the 2D scattering pattern, and the data in the angular range of $0.007 < q < 0.15$ Å^{-1} was used as the SAXS pattern, in which $q = 4\pi\sin\theta/\lambda$ (where 2θ is the scattering angle and λ is the wavelength of the X-ray source) (Zhang et al., 2014; Zhang, Chen, Li, Li, & Zhang, 2015a). All data was background subtracted and normalised. The starch-based films were placed on a multi-well stage provided by the Australian Synchrotron, and then the SAXS data recorded for an acquisition time of 1 s.

2.3.6. Fourier-transform infrared (FT-IR) spectroscopy

The FT-IR spectra of different starch samples were recorded using a Nicolet 5700 FT-IR spectrometer (Thermo Electron Corporation, Madison, WI, USA) equipped with a Nicolet Smart Orbit attenuated total reflectance (ATR) accessory incorporating a diamond internal reflection element. For

each spectrum, 64 scans were recorded over the range of 4000–600 cm^{-1} at RT (about 22 °C) at a resolution of 4 cm^{-1}, co-added and Fourier-transformed. The background spectrum was recorded on air and subtracted from the sample spectrum. FT-IR spectra were baseline corrected and normalised using the band at 995 cm^{-1} before further analysis.

2.3.7. Fourier-transform Raman (FT-Raman) spectroscopy

The FT-Raman spectra were performed on an FT-Raman Module (NXR, Thermo Fisher Scientific, Madison, WI, USA). The Raman optics system comprised a Nd:YVO4 laser operating at 1064 nm, sample holders, an InGaAs (Indium-Gallium Arsenide) detector, and a CaF_2 beam splitter. Spectra of starches placed in the sample holder were collected with a laser power of 0.77–0.82 W, a mirror velocity of 0.3165 $cm \cdot s^{-1}$, and 256 scans at a resolution of 16 cm^{-1}. Spectra were obtained in the Raman shift range between 400 and 3400 cm^{-1} using OMNIC software (version 5.1, Thermo Electron Corporation, Madison, WI, USA).

3. Results and Discussion

3.1. Moisture uptake during ageing

The moisture uptake of [Emim][OAc]- and glycerol-plasticised starch-based films was monitored during storage at 33% and 75% RH's (Fig. 1). We observe from Fig. 1 that all the films presented similar moisture uptake behaviour. The moisture uptake increased rapidly at the beginning (especially during the first week) then gradually slowed down. And after two weeks, the moisture uptake levelled off.

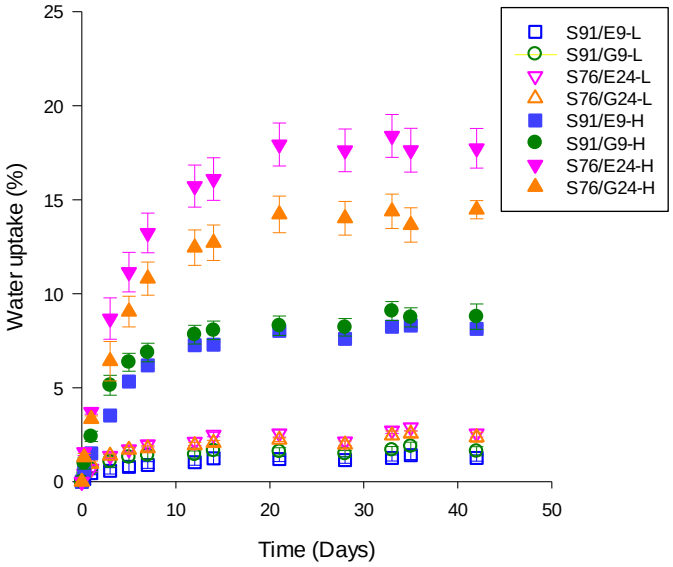

Fig. 1 Moisture uptake results of the different starch-based films after ageing at 33% (L) or 75% (H) relative humidity.

The degree of moisture uptake was drastically influenced by the plasticiser type and content. Generally, higher plasticiser content and/or higher RH during storage led to higher final moisture uptake; and, the presence of IL resulted in higher water uptake than the presence of glycerol plasticiser (for the same amount of plasticiser). Albeit at low amount of plasticiser level, there was no significant difference between the IL- and glycerol-plasticised samples. The greatest degree of final moisture uptake was observed for S76/E24-H (17.7±1.1%) and then S76/G24-H (14.5±0.5%) (Fig. 1 and Table 1), indicating the strong ability of the non-volatile plasticisers ([Emim][OAc] stronger than glycerol) to bind with moisture from the environment. However, at 33% (L) RH, the same samples could only achieve 2.6±0.2% (for S76/E24-L) and 2.4±0.3% (for S76/G24-L), suggesting that limited moisture was absorbed from the environment in this case. In contrast, S91/E9-H and S91/G9-H still achieved 8.1±0.2% and 8.8±0.7% water uptake. As usual for polysaccharide-based materials, we can see that the moisture

content was mainly influenced by the plasticiser (glycerol or [Emim][OAc]), which has a hydrophilic nature and interacts through hydrogen bonding both with starch hydroxyls and water molecules, and logically by the storage RH.

The final compositions including moisture content of samples after storage for 42 days are shown in Table 1, which are useful for the following discussion.

3.2. Mechanical properties

Fig. 2 shows the tensile mechanical properties of different starch samples before and after ageing. Before ageing, the samples with low plasticiser content (S91/E9 and S91/G9) exhibited much higher σ_t and E and much lower ε_b than the samples with high plasticiser content (S76/E24 and S76/G24). This was not surprising regarding the plasticisation effect of plasticisers ([Emim][OAc] and glycerol), which are stronger than water. Both [Emim][OAc] and glycerol could result in partial disruption of hydrogen bonding between starch molecules, forming hydrogen bonds with the –OH sites of starch. Considering [Emim][OAc] and glycerol are bigger molecules than water, these two plasticisers might act more effectively to increase the free volume of the starch macromolecules, resulting in more reduced strength and stiffness. Also, the plasticisers prevented macromolecular entanglement, resulting in less "connections" between the polymer chains, as demonstrated by higher ε_b.

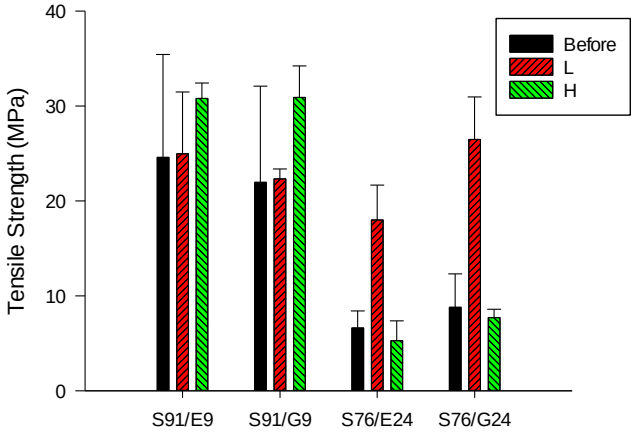

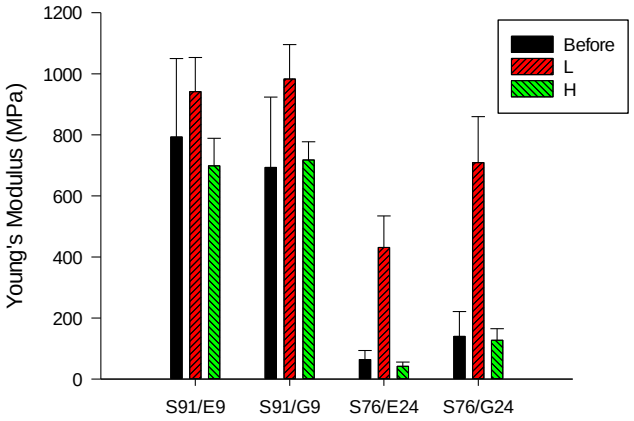

(a) (b)

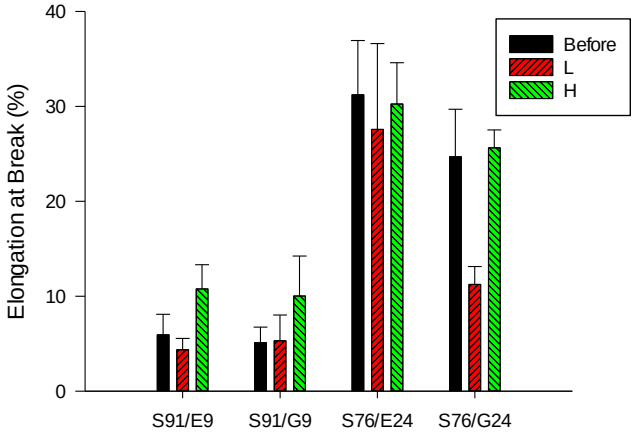

(c)

Fig. 2 Tensile strength (σ_t) (a), Young's modulus (E) (b), and elongation at break (ε_b) (c) of the different starch-based films either before ageing, or after ageing at 33% (L) or 75% (H) relative humidity.

In addition, S76/E24 showed lower σ_t and E and higher ε_b than S76/G24. This was as expected since [Emim][OAc] has a stronger plasticisation effect than glycerol due to its greater ability to disrupt

hydrogen boding (Xie et al., 2014). However, a low amount of plasticiser did not result in significant differences in mechanical properties between glycerol- and IL-plasticised samples (S91/E9 and S91/G9).

Ageing could affect σ_t, E and ε_b to different extents, depending on the plasticiser type and content in the sample, and the RH during storage (Fig. 2). It can be seen that for both S76/E24 and S76/G24, σ_t and E experienced little variations after ageing at 75% (H) RH, but increased strongly at 33% (L) RH. It could be possible that when the storage RH was 33% which only slightly changed the moisture content (see Fig. 1), densification (in amorphous regions, below glass transition temperature (Xie et al., 2014)) occurred (Xie et al., 2013). 75% RH might result in the moisture contents in S76/E24 and S76/G24 being too high (see Fig. 1) to make any densification during ageing possible. Densification could be easier with glycerol which could be seen by a big decrease in ε_b for S76/G24 at 33% (L) RH.

On the other hand, for both S91/E9 and S91/G9, no statistically significant changes to σ_t and E were observed irrespective of the storage RH (Fig. 2). This might suggest that with limited plasticiser content (either [Emim][OAc] or glycerol) the addition of (limited) water during ageing did not result in apparent densification. Nonetheless, more water might decrease the stiffness and soften the material, as we could observe a slight decrease in E and moderate increase in ε_b for S91/E9 and S91/G9 aged at 75% (H) RH.

The variations in mechanical properties among different samples seemed to mainly relate to the amorphous starch in samples as influenced by the plasticiser, which dominated the influence from the differences in crystallinity. This will be discussed in Section 3.4.

3.3. TGA

For a thorough understanding of the thermal decomposition of different starch-based films, the TGA of pure [Emim][OAc] and glycerol and their mixtures with water were firstly carried out (Fig. 3a). It can be seen that pure [Emim][OAc] had a big derivative weight loss peak between about 160 °C and

275 °C, showing its thermal decomposition. This temperature range of TGA decomposition is exactly in agreement with a previous study which documented the lower thermal stability of acetate IL's than IL's containing other anions like [Cl^-] (Wendler, Todi, & Meister, 2012). In addition, starting from about 75 °C, there was a slight weight loss immediately before the decomposition, which might be ascribed to the evaporation of impurities present in the starting materials (< 5%, mainly acetic acid, methylimidazol, and water). The 9:1 (wt/wt) [Emim][OAc]:water solution had a TGA profile very similar to pure [Emim][OAc] except that the weight loss was more apparent and at a lower temperature. The TGA curve of 3:7 (wt/wt) [Emim][OAc]:water solution showed a much sharper and intensified peak at about 95 °C, which can be undoubtedly attributed to water evaporation, because of the large amount of water contained in this solution. The 3:7 (wt/wt) [Emim][OAc]:water solution also had a thermal decomposition peak at the same position as that of pure [Emim][OAc] but the intensity was reduced.

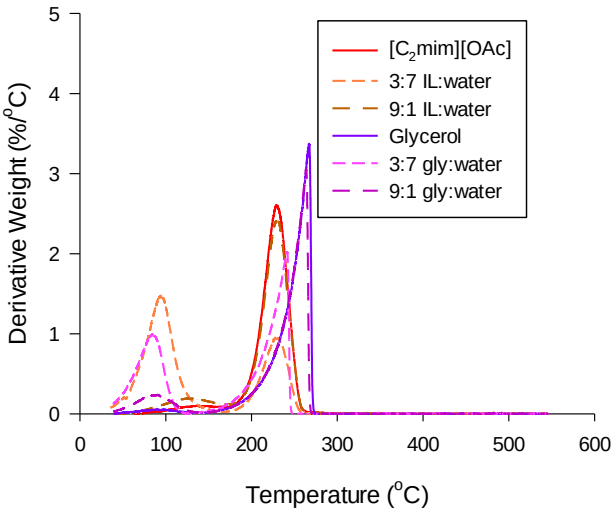

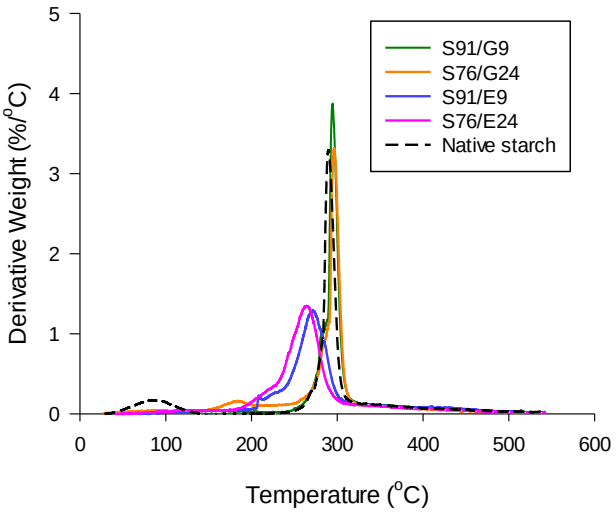

(a) (b)

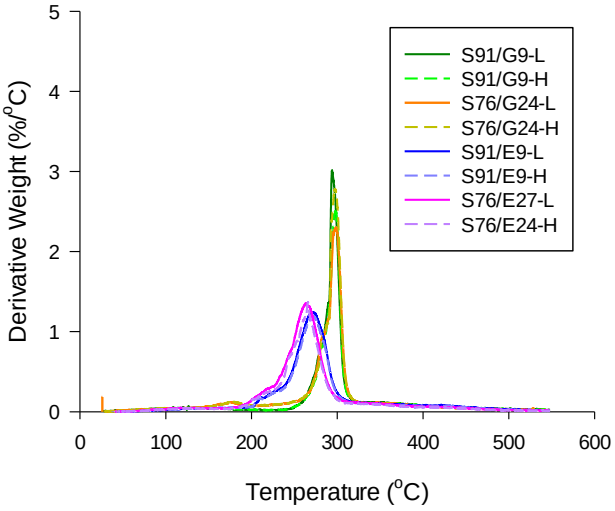

(c)

Fig. 3 TGA curves of pure [Emim][OAc], 9:1 (wt/wt) [Emim][OAc]:water solution, 3:7 (wt/wt) [Emim][OAc]:water solution, pure glycerol, 9:1 (wt/wt) glycerol:water solution, 3:7 (wt/wt) glycerol:water solution (a); native Gelose 80 starch, and the different starch-based films before ageing (b); and these films after ageing at either low (33%) and high (75%) relative humidity (c).

Also from Fig. 3a, pure glycerol had a very sharp peak at 265 °C, starting as early as 140 °C but ending immediately after the peak, due to the thermal decomposition of glycerol. The glycerol decomposition (peak) temperature was previously detected at *ca.* 245 °C while using a higher heating ramp (15 K/min) (Jackson & Rager, 2001). With the inclusion of water, the 9:1 (wt/wt) glycerol:water solution and the 3:7 (wt/wt) glycerol:water solution had a prominent peak from *ca.* 45 °C until 130 °C, which was not surprising and was due to water evaporation. Interestingly, the thermal decomposition peak of 3:7 (wt/wt) glycerol:water solution was reduced to 241 °C, which was 26 °C lower than that of pure glycerol. It is proposed that there were some water molecules that are strongly bound to glycerol and this binding reduced the thermal decomposition of glycerol.

Fig. 3b shows the TGA results of the four starch-based films before ageing, as well as native starch. For native starch, there was a weight loss between about 40 °C and 140 °C, due to the evaporation of moisture contained in starch. After that, the thermal decomposition of starch occurred between about 240 °C and 330 °C, corresponding well with previous studies (Liu, Yu, Liu, Chen, & Li, 2009b; Liu et al., 2010). This main peak could be specifically associated with the breakage of long chains of starch as well as the destruction (oxidation) of the glucose rings (Liu et al., 2009b). After the processing of starch, S91/G9 and S76/G24 displayed a very similar thermal decomposition to that of native starch. For S91/G9, the thermal decomposition peak for glycerol was not observable, as it was overlapped by the thermal decomposition peak for starch. But for S76/G24, there was an apparent weight loss between about 150 °C and 200 °C followed by stable and continuous weight loss extending into the starch decomposition peak. This loss from 150 °C was also visible in previous studies of glycerol-plasticised starch-based materials (Chiou et al., 2007; Wilhelm, Sierakowski, Souza, & Wypych, 2003; Xie et al., 2014), and was attributed to the thermal decomposition to starch-glycerol (Wilhelm et al., 2003).

It can also be seen from Fig. 3b that starch plasticised by [Emim][OAc] had reduced thermal stability, as the maximum rate of weight loss (derivative peak) occurred at 271 °C and 263 °C for S91/E9 and S76/E24 respectively, compared with native starch at 290 °C. This also meant the greater the amount of [Emim][OAc], the lower was the thermal stability of starch. As this main TGA peak spanned from 185 °C to 330 °C, it should have overlapped the thermal decomposition of [Emim][OAc] (see Fig. 3a).

Fig. 3c displays the TGA results of the four starch-based films after ageing. Comparing Fig. 3c with Fig. 3b, it can be seen that ageing did not apparently influence the thermal decomposition profile. Also, no distinct difference was seen for the same sample after ageing at different RH. Thus, it can be concluded that, irrespective of the ageing process and the moisture uptake, the thermal decomposition temperature of starch-based films only depended on the plasticiser type and content — [Emim][OAc] had an obvious effect in reducing the thermal stability of starch-based materials; but glycerol did not have such an effect. This is in agreement with our previous reports (Xie et al., 2014; Xie et al., 2015).

3.4. XRD

Fig. 4 shows the XRD patterns of native starch and the different starch-based films. Native G80 showed a strong diffraction peak at a 2θ position of about 17°, with a few smaller peaks at 2θ of about 5.5°, 10.0°, 14.8°, 17.0°, 22.1°, 23.8°, and 26.1°, indicative of B-type crystalline structure (Cheetham & Tao, 1998; Tan et al., 2007). After processing, besides the original B-type characteristic peaks (main peak at $2\theta \approx 17°$, with much lower intensity though), all the starch samples, both before and after ageing, displayed peaks at 2θ of about 7.3°, 12.7°, 19.5°, and 22.2°, characteristic of V_H-type crystalline structure, a single-helical amylose structure (similar to that formed by amylose–lipid helical complexes) and is well known for thermally-processed (*e.g.*, compression moulding and extrusion) starch-based

materials (van Soest et al., 1996). That is, the plasticised samples contained crystalline structure and were not destructured by compression moulding (which is normal in starch processing) and some newly formed V_H-type crystalline structure mainly induced by processing (van Soest et al., 1996; van Soest & Borger, 1997).

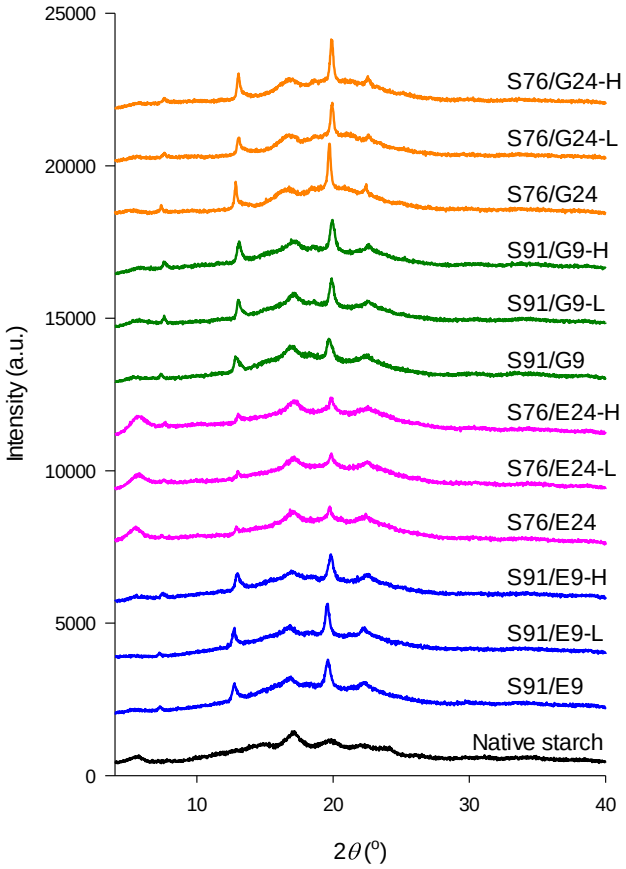

Fig. 4 XRD results of native G80 starch, and the different starch-based films either before ageing, or after ageing at 33% (L) and 75% (H) relative humidity.

The crystallinity of the samples calculated from the XRD patterns is shown in Table 2. It seems that ageing didn't have any apparent impact on the degree of crystallinity (both B-type and V-type) regardless of the plasticiser type and content, which was surprising. The V-type crystallites were mostly formed during compression moulding and no new B-type crystallites was generated during ageing.

[Insert Table 2 here]

It can be seen from Table 2 that, unlike the other samples (with E9, G9 and G27), V-type crystalline structure could hardly be newly generated for S76/E24 during compression moulding. It is suggested that when a large amount of starch hydroxyls were bound with the IL, the formation of helices might be difficult due to steric hindrance. Single helices of starch are formed via hydrogen bonding between the O3' and O2 oxygen atoms of sequential residues. Additionally, a helical amylose has hydrogen-bonding O2 and O6 atoms on the outside surface of the helix, forming a double-helical structure via hydrogen bonding of two strand-adjacent glucose molecules and holding the two strands of the double helix together. It is proposed that the effect of hindering either helix formation was due to the strong interaction between the acetate anion in [Emim][OAc] and starch hydroxyl groups, disrupting hydrogen bonding in the starch polymer and making it difficult for the amylose molecules to form single (and double) helices. On the other hand, while S91/E9, S91/G9 and S76/G24 had similar degrees of V-type crystallinity (about 5%), S76/G24 displayed sharper peaks at 20° (see Fig. 4). Thus, a higher content of glycerol could lead to larger and better V-type crystals (Xie et al., 2014).

It is also noticeable in Table 2 that compared with S91/G9, S91/E9 had lower B-type crystallinity, which was even lower than those plasticised by E24. Possibly, during compression moulding, a mixture of [Emim][OAc] and water can better diffuse into starch granules and disrupt the starch hydrogen bonding, due to reduced viscosity and an synergistic effect (Mateyawa et al., 2013).

Therefore, due to higher amounts of both B-type and V-type crystallites in glycerol-plasticised samples, they were less amorphous than [Emim][OAc]-plasticised starch (Xie et al., 2014). Nonetheless in this study, no evident relationship between the crystallinity and mechanical properties could be established. Probably, the mechanical properties seemed more strongly influenced by the plasticisation on the amorphous parts, as well as the densification of amorphous starch during ageing, as discussed in Section 3.2.

3.5. Synchrotron SAXS

Fig. 5a shows the synchrotron SAXS patterns of native starch and the different starch-based films before ageing. After Lorentz-correction (Fig. 5b), the pattern characteristics could be more clearly displayed.

Expectedly, native starch displayed a typical SAXS peak at a q range of *ca.* 0.06–0.07 $Å^{-1}$, corresponding to the semi-crystalline lamellar structure of starch (Zhang, Li, Liu, Xie, & Chen, 2013; Zhang et al., 2015b). Upon processing by compression moulding, for S91/G9 and S91/E9, the semi-crystalline lamellar structure was completely lost, accompanied by the emergence of an inflection of the SAXS pattern at a lower q range. This inflection, correlated to the Guinier scattering behaviour (*i.e.*, a structure with a certain radius of gyration) (Beaucage, 2004), could be attributed to a gel-like structure on nano-scale (mean square radius of gyration: *ca.* 25 nm) constituted by amorphous starch and plasticiser molecules ([Emim][OAc] or glycerol). It is noted that the inflection for S91/E9 was less

apparent than that for S91/G9, indicating greater homogeneity of the [Emim][OAc]-plasticised starch. This was consistent with the higher amorphous content of S91/E9 (XRD results in Table 2).

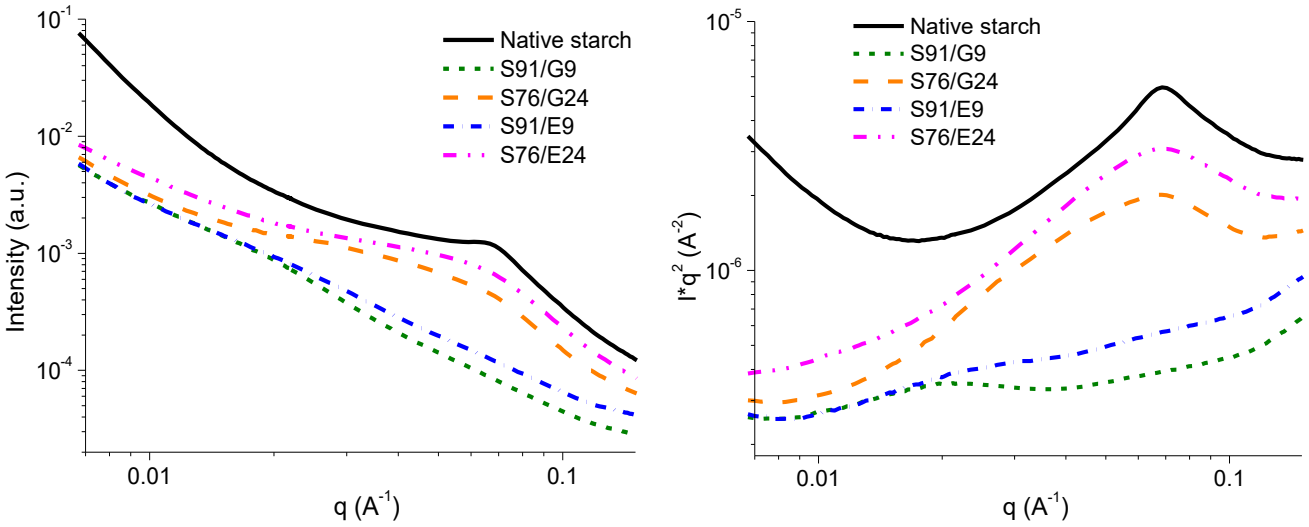

(a) (a)

Fig. 5 Synchrotron SAXS results (a), and their Lorentz-corrected patterns (b), for native G80 starch and different starch-based films before ageing.

With the inclusion of a greater amount of plasticiser, while no lamellar peak (like the one for native starch) was shown for S76/G24 and S76/E24, a "shoulder" (indicative of molecular order on the nanoscale (Lopez-Rubio, Htoon, & Gilbert, 2007)) was displayed for both samples at a *q* range similar to that for the native starch lamellar peak. Compared to the lamellar peak, the shoulder was broader and less defined, due to a broad distribution of molecular organisation in those two samples. By associating the SAXS results with the XRD data, it was found that although there was always a certain amount of crystallites (molecular order) in the plasticised starch, the alignment of starch crystallites in a certain

distribution range on the nanoscale only preferably occurred with a higher amount of plasticiser (*i.e.*, for S76/G24 or S76/E24). This could be attributed to enhanced plasticisation of the flexible spacers (such as the amorphous amylopectin branching points) in the starch-based films (Daniels & Donald, 2004; Vermeylen et al., 2006). Besides, S76/G24 had a wider shoulder than S76/E24, accompanied by an inflection at *ca.* 0.03 $Å^{-1}$, suggesting that S76/G24 had not only broadly distributed molecular order, but also contained a gel-like structure similar to that in S91/G9 and S91/E9. This again confirmed that, compared with glycerol, [Emim][OAc] could eventually make the starch-based film more homogenous with lower distribution range of molecular order and without gel-aggregated structure on the nanoscale.

Fig. 6 shows the Lorentz-corrected synchrotron SAXS patterns of the different starch-based films before and after ageing. It is seen that ageing did not substantially affect the SAXS patterns for S91/G9 and S91/E9, suggesting no significant changes in their crystalline and amorphous regions on the nanoscale. Nonetheless, a slight decrease in the overall scattering intensity for S91/G9-L and S91/E9-L could be observed, indicating a reduced electron difference between the crystalline and amorphous regions. To account for this, it is proposed that, at 33% (L) RH, the small amount of water trapped in S91/G9 or S91/E9 during ageing (see Table 1) should preferentially bond with glycerol or [Emim][OAc], thus weakening the interactions between starch hydroxyls and the plasticiser. This might assist in macromolecular entanglements and thus densification (*i.e.*, increased electron density), especially in the amorphous region of plasticised starch. When the RH was 75% (H), S91/E9-H presented a less evident decrease in the overall scattering intensity, while S91/G9-H showed decreased intensity at $q < 0.03$ $Å^{-1}$ but increased intensity at $q > 0.03$ $Å^{-1}$. It was possible that the increased amount of water resulting from a higher RH also acted like a “plasticiser” for the starch-based materials, weakening the structural densification. From all these results, we can conclude that, during ageing (especially at a lower RH), the

starch-based films containing a small amount of plasticiser (S91/E9 and S91/G9) was somewhat unstable and thus underwent slight alterations to its nanoscale structure.

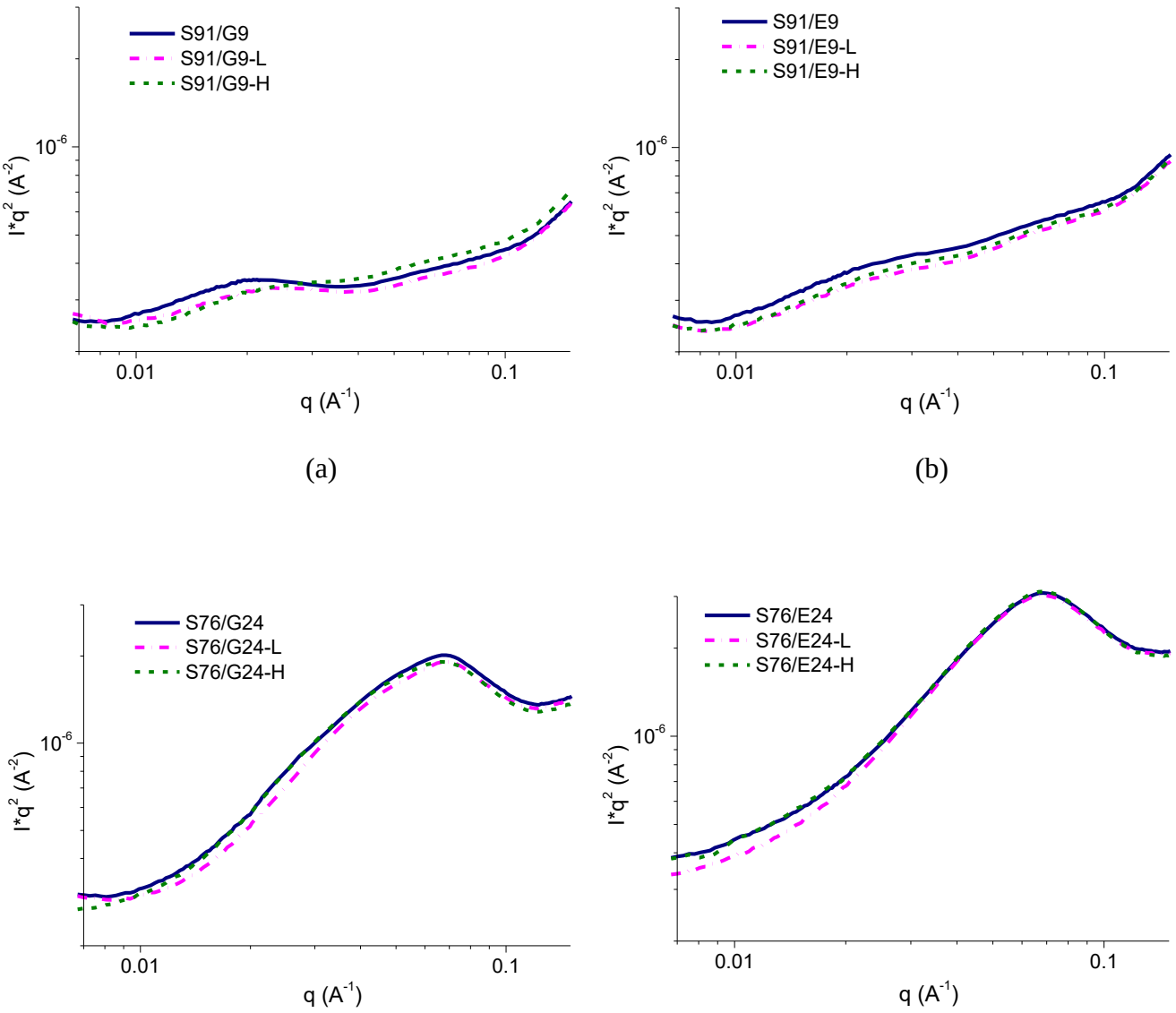

Fig. 6 Lorentz corrected synchrotron SAXS results of the different starch-based films either before ageing, or after ageing at 33% (L) and 75% (H) relative humidity.

On the other hand, S76/G24-H showed a very weak decrease in scattering intensity at some *q* region, whereas S76/G24-L had a greater intensity reduction at overall *q* region. This means that compared with ageing at a high RH, low-RH ageing could more effectively induce nano-structural densification, in particular for the amorphous region, of the plasticised starch with a high amount of glycerol. However, for S76/E24, we could not see any changes in the scattering intensity after ageing at 75% (H) RH. Even after ageing at 33% (L) RH, S76/E24-L only presented a very small intensity reduction in the limited range of $q < 0.03$ Å^{-1}. The less apparent nano-structural evolution of S76/E24 during ageing clearly demonstrate that, compared to glycerol, the IL made the plasticised starch much more stable at different RH's.

Hence, from a nano-structural perspective, we have shown that [Emim][OAc] has an excellent plasticisation effect on starch, which can be demonstrated by increased homogeneity in [Emim][OAc]-plasticised starch as compared to glycerol-plasticised starch (*i.e.*, less gel-like aggregates, and narrower distribution of aligned crystallites); Moreover, during ageing, the IL was more effective at preventing densification (especially in the amorphous starch) and thus provided starch-based materials with a greater ageing-stability. This has a strong link to the materials properties such as mechanical properties.

3.6. FT-IR spectroscopy

FT-IR spectroscopy was used to probe the potential changes in molecular interactions in the starch-based films. Compared with the IR bands of native starch, the starch-based films mainly showed differences in the ranges of 1700–1200 cm^{-1} and 3700–2700 cm^{-1} (Fig. 7a and Fig. 7b, respectively). In Fig. 7a, the IL showed two characteristic IR absorption peaks at *ca.* 1380 cm^{-1} and 1580 cm^{-1} respectively, corresponding to the symmetric and asymmetric O–C–O stretches of the [OAc]$^{-}$ anion of

559 IL (Delgado, Rodes, & Orts, 2007; Zhang et al., 2015b), and expectedly no O–C–O stretch IR peaks
560 emerged in the range of 1700–1200 cm^{-1} for glycerol. Thus, after processing by compression moulding,
561 while glycerol-plasticised starch-based films had no substantial band alterations at 1700–1200 cm^{-1},
562 [Emim][OAc]-plasticised ones displayed two slightly shifted IR absorption peaks of O–C–O stretches at
563 *ca.* 1400 cm^{-1} and 1560 cm^{-1}, respectively. The hydroxyl absorption peak at *ca.* 3300 cm^{-1} was slightly
564 shifted left; and this shift indicates that the plasticiser molecules interacted with starch hydroxyl groups
565 presumably through hydrogen bonding. However, S76/E24 displayed a prominent decrease in the
566 hydroxyl absorption peak, due to the intense hydrogen bonding between [Emim][OAc] and starch, as
567 shown in our previous findings (Zhang et al., 2015b). This could be verified by the emergence of a
568 second hydroxyl peak at *ca.* 3160 cm^{-1} resulting from hydrogen bonding effects by the IL.
569

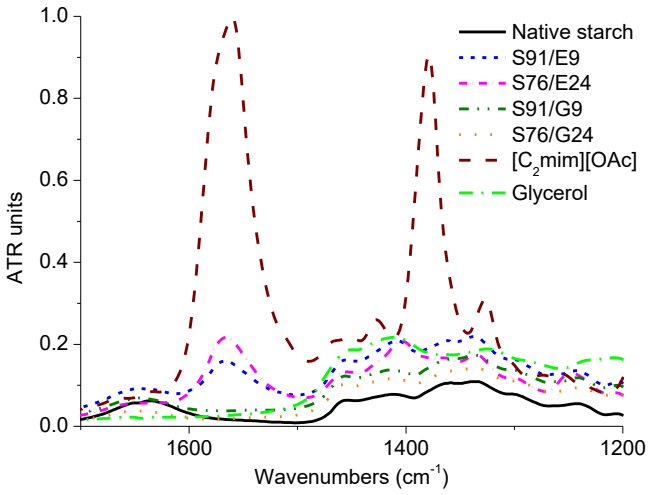

(a)

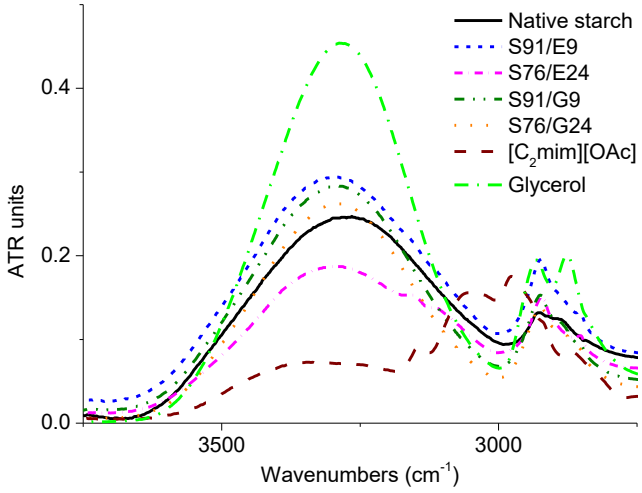

(b)

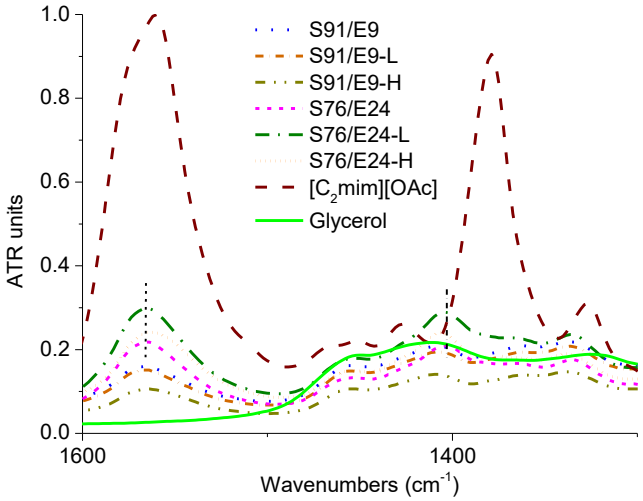

(c)

Fig. 7 FT-IR spectra of native G80 starch (a and b), [Emim][OAc] (a, b, and c), glycerol (a, b, and c) and different starch-based films before ageing (a, b), or after ageing (c) at 33% (L) and 75% (H) relative humidity.

581 Since those two peaks for $[OAc]^-$ at *ca.* 1400 cm^{-1} and 1560 cm^{-1} were much sharper than the peak
582 for hydroxyls at *ca.* 3300 cm^{-1}, the former were further focused on in an attempt to understand the
583 ageing-induced evolution of molecular interactions in [Emim][OAc]-plasticised starch. As seen from
584 Fig. 7c, after ageing, although no notable shifting of the two O–C–O stretch bands were observed for
585 S91/E9-L, S91/E9-H, and S76/E24-L, the peaks at 1400 cm^{-1} and 1560 cm^{-1} for S76/E24-H slightly
586 shifted left and right, respectively, indicative of certain hydrogen bonding between the IL and water
587 molecules (Zhang et al., 2015b). This revealed that the water molecules adsorbed from the environment
588 during ageing could interact with the plasticiser and thus induce structural changes (typically
589 densification on the nanoscale), despite that this could not be apparently detected under certain
590 conditions, *e.g.*, low plasticiser content and/or low RH.
591
592 *3.7. Raman spectroscopy*
593 For further confirmation of the ageing-induced evolution of molecular interactions in plasticised
594 starch, Fig. 8 shows the Raman spectra of native starch, the IL, glycerol, and the different starch-based
595 films without and with ageing. By comparing the Raman spectra of different plasticised starch samples
596 with those of native starch, the IL, and glycerol, starch-based films plasticised by glycerol (both at high
597 and low contents) were found to exhibit predominantly typical starch-like Raman bands at different
598 wavenumbers, but those plasticised by [Emim][OAc] did not display such bands but instead showed
599 several broad peaks, similar to the Raman spectrum of fully-gelatinised starch (Kizil & Irudayaraj, 2005).
600 This further demonstrated that the IL was effective to interact with starch and thus preventing starch
601 molecular interactions (*e.g.*, entanglement and crystallisation). Besides, after ageing, none of the starch-
602 based films presented apparent changes in the Raman spectra, indicating no ageing-induced alterations
603 to starch molecular interactions in the starch-based films. In other words, [Emim][OAc] could not only

sufficiently plasticise starch and make starch molecular interactions similar to those in gelatinised starch, but also effectively keep this plasticised state during ageing.

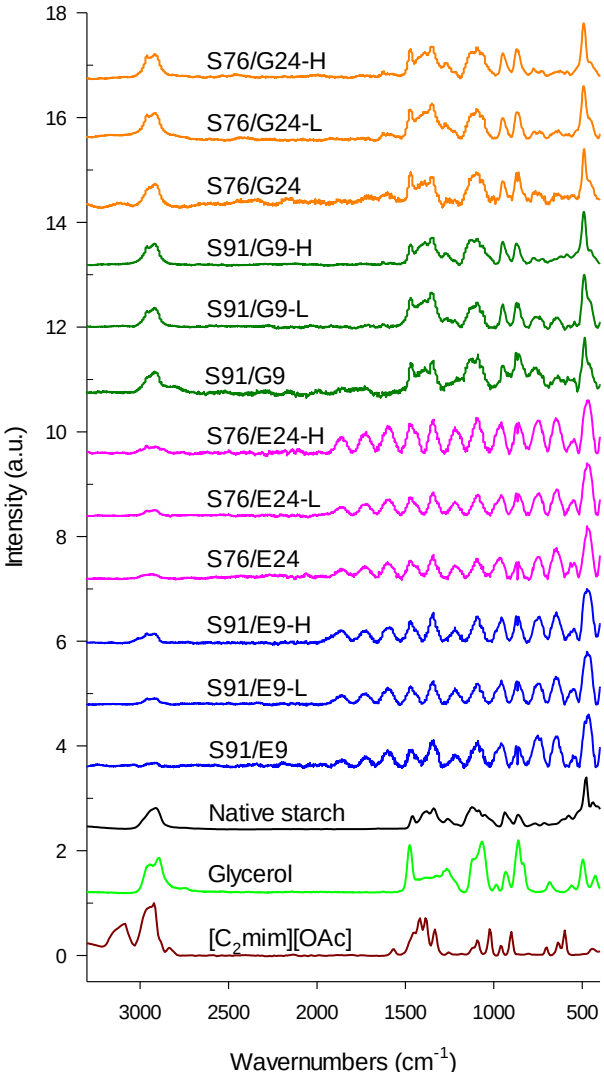

Fig. 8 Raman spectra of native G80 starch, [Emim][OAc], glycerol, and different starch-based films either before ageing, or after ageing at 33% (L) and 75% (H) relative humidity.

4. Conclusion

By investigation on multiple length scales, this study demonstrated that [Emim][OAc] could result in greater homogeneity in starch-based materials than glycerol. While both plasticisers at high content could lead to well-plasticised starch during processing, [Emim][OAc] due to its stronger ability to interact with starch molecules, would more effectively destructurise the starch supramolecular structure, resulting in greater homogeneity in the starch-based films. In particular, the [Emim][OAc]-plasticised starch-based films did not show any gel-like aggregate features and contained less molecular order (crystallites) in a reduced distribution range on the nanoscale. Moreover in this case, there were much weaker starch-starch interactions but stronger starch-[Emim][OAc] interactions at the molecular level, which resulted in reduced strength and stiffness but increased flexibility of the films.

More importantly, this work also revealed that [Emim][OAc] could more effectively maintain the plasticised state during ageing than glycerol. With plasticisation by [Emim][OAc], densification (especially in the amorphous regions) could be suppressed, presumably due to the fact that the IL sufficiently plasticised starch, resulting in starch molecular interactions similar to those in gelatinised starch, and effectively keep this plasticised state during ageing. In particular, if the starch-based film was plasticised by a high [Emim][OAc] content, its structural characteristics especially on the nanoscale were quite stable especially at a high RH (and only showed slight changes at a low RH). This could contribute to the stabilised mechanical properties.

Considering the excellent conducting behaviours of IL's (Ramesh et al., 2011a; Wang et al., 2009a), our investigation provides possibilities to develop 'green' electroactive or electro-conductive starch-based materials with excellent plasticisation and stability for real applications (e.g. smart devices, and biosensors). These applications will be more practically meaningful if the cost of the IL is further reduced by improving the IL production with more efficient and cost-effective industrial approaches.

636 Also, as starch is a typical semi-crystalline bio-polymer containing a large number of hydroxyls
637 (involving strong inter- and intra-molecular hydrogen bonding), this work should be of value in the
638 rational development of new methods based on IL's to process more semi-crystalline natural polymers
639 (*e.g.*, cellulose, dextrin and xylan) other than starch.
640
641
642 **Acknowledgements**
643 The research leading to these results has received funding from the Australian Research Council
644 (ARC) under the Discovery Project No. 120100344. It has also been supported by the Open Project
645 Program of Guangdong Province Key Laboratory for Green Processing of Natural Products and Product
646 Safety. The SAXS/WAXS measurements were performed at the Australian Synchrotron, Victoria,
647 Australia. B. Zhang also would like to thank the China Scholarship Council (CSC) for providing
648 financial support for his visiting studies at The University of Queensland (UQ) as part of his Ph.D. work.
649
650 **References**
651 Avérous, L. (2004). Biodegradable multiphase systems based on plasticized starch: a review. *Polymer*
652 *Reviews, 44*(3), 231-274.
653 Beaucage, G. (2004). Determination of branch fraction and minimum dimension of mass-fractal
654 aggregates. *Physical Review E: Statistical, Nonlinear, and Soft Matter Physics, 70*(3), 031401.
655 Bendaoud, A., & Chalamet, Y. (2013). Effects of relative humidity and ionic liquids on the water
656 content and glass transition of plasticized starch. *Carbohydrate Polymers, 97*(2), 665-675.

Biswas, A., Shogren, R. L., Stevenson, D. G., Willett, J. L., & Bhowmik, P. K. (2006). Ionic liquids as solvents for biopolymers: Acylation of starch and zein protein. *Carbohydrate Polymers, 66*(4), 546-550.

Cheetham, N. W. H., & Tao, L. (1998). Variation in crystalline type with amylose content in maize starch granules: an X-ray powder diffraction study. *Carbohydrate Polymers, 36*(4), 277-284.

Chiou, B.-S., Wood, D., Yee, E., Imam, S. H., Glenn, G. M., & Orts, W. J. (2007). Extruded starch-nanoclay nanocomposites: effects of glycerol and nanoclay concentration. *Polymer Engineering & Science, 47*(11), 1898-1904.

Daniels, D. R., & Donald, A. M. (2004). Soft material characterization of the lamellar properties of starch: Smectic side-chain liquid-crystalline polymeric approach. *Macromolecules, 37*(4), 1312-1318.

Delgado, J. M., Rodes, A., & Orts, J. M. (2007). B3LYP and in situ ATR-SEIRAS study of the infrared behavior and bonding mode of adsorbed acetate anions on silver thin-film electrodes. *The Journal of Physical Chemistry C, 111*(39), 14476-14483.

El Seoud, O. A., Koschella, A., Fidale, L. C., Dorn, S., & Heinze, T. (2007). Applications of ionic liquids in carbohydrate chemistry: A window of opportunities. *Biomacromolecules, 8*(9), 2629-2647.

Farhat, I. A., Blanshard, J. M. V., & Mitchell, J. R. (2000). The retrogradation of waxy maize starch extrudates: Effects of storage temperature and water content. *Biopolymers, 53*(5), 411-422.

Forssell, P. M., Hulleman, S. H. D., Myllärinen, P. J., Moates, G. K., & Parker, R. (1999). Ageing of rubbery thermoplastic barley and oat starches. *Carbohydrate Polymers, 39*(1), 43-51.

678 Fu, Z.-q., Wang, L.-j., Li, D., Wei, Q., & Adhikari, B. (2011). Effects of high-pressure homogenization
679 on the properties of starch-plasticizer dispersions and their films. *Carbohydrate Polymers, 86*(1),
680 202-207.
681 Heinze, T., Schwikal, K., & Barthel, S. (2005). Ionic liquids as reaction medium in cellulose
682 functionalization. *Macromolecular Bioscience, 5*(6), 520-525.
683 Jackson, R. S., & Rager, A. (2001). The use of reduced pressure to expand the capabilities of TGA–
684 FTIR. *Thermochimica Acta, 367–368*, 415-424.
685 Jane, J.-l. (2009). Structural features of starch granules II. In B. James, & W. Roy (Eds.), *Starch (Third*
686 *Edition)* (pp. 193-236). San Diego: Academic Press.
687 Kizil, R., & Irudayaraj, J. (2005). Discrimination of irradiated starch gels using FT-raman spectroscopy
688 and chemometrics. *Journal of Agricultural and Food Chemistry, 54*(1), 13-18.
689 Leroy, E., Jacquet, P., Coativy, G., Reguerre, A. l., & Lourdin, D. (2012). Compatibilization of starch–
690 zein melt processed blends by an ionic liquid used as plasticizer. *Carbohydrate Polymers, 89*(3),
691 955-963.
692 Liew, C.-W., Ramesh, S., Ramesh, K., & Arof, A. (2012). Preparation and characterization of lithium
693 ion conducting ionic liquid-based biodegradable corn starch polymer electrolytes. *Journal of Solid*
694 *State Electrochemistry, 16*(5), 1869-1875.
695 Liew, C.-W., & Ramesh, S. (2015). Electrical, structural, thermal and electrochemical properties of corn
696 starch-based biopolymer electrolytes. *Carbohydrate Polymers, 124*(0), 222-228.
697 Liu, H., Xie, F., Yu, L., Chen, L., & Li, L. (2009a). Thermal processing of starch-based polymers.
698 *Progress in Polymer Science, 34*(12), 1348-1368.
699 Liu, X., Yu, L., Liu, H., Chen, L., & Li, L. (2009b). Thermal decomposition of corn starch with different
700 amylose/amylopectin ratios in open and sealed systems. *Cereal Chemistry, 86*(4), 383-385.

Liu, X., Yu, L., Xie, F., Li, M., Chen, L., & Li, X. (2010). Kinetics and mechanism of thermal decomposition of cornstarches with different amylose/amylopectin ratios. *Starch/Stärke, 62*(3-4), 139-146.

Lopez-Rubio, A., Htoon, A., & Gilbert, E. P. (2007). Influence of extrusion and digestion on the nanostructure of high-amylose maize starch. *Biomacromolecules, 8*(5), 1564-1572.

Lopez-Rubio, A., Flanagan, B. M., Gilbert, E. P., & Gidley, M. J. (2008). A novel approach for calculating starch crystallinity and its correlation with double helix content: A combined XRD and NMR study. *Biopolymers, 89*(9), 761-768.

Mateyawa, S., Xie, D. F., Truss, R. W., Halley, P. J., Nicholson, T. M., Shamshina, J. L., et al. (2013). Effect of the ionic liquid 1-ethyl-3-methylimidazolium acetate on the phase transition of starch: Dissolution or gelatinization? *Carbohydrate Polymers, 94*(1), 520-530.

Pérez, S., Baldwin, P. M., & Gallant, D. J. (2009). Structural features of starch granules I. In B. James, & W. Roy (Eds.), *Starch (Third Edition)* (pp. 149-192). San Diego: Academic Press.

Pérez, S., & Bertoft, E. (2010). The molecular structures of starch components and their contribution to the architecture of starch granules: a comprehensive review. *Starch/Stärke, 62*(8), 389-420.

Phillips, D. M., Drummy, L. F., Conrady, D. G., Fox, D. M., Naik, R. R., Stone, M. O., et al. (2004). Dissolution and regeneration of bombyx mori silk fibroin using ionic liquids. *Journal of the American Chemical Society, 126*(44), 14350-14351.

Pu, Y., Jiang, N., & Ragauskas, A. J. (2007). Ionic liquid as a green solvent for lignin. *Journal of Wood Chemistry and Technology, 27*(1), 23-33.

Qin, Y., Lu, X., Sun, N., & Rogers, R. D. (2010). Dissolution or extraction of crustacean shells using ionic liquids to obtain high molecular weight purified chitin and direct production of chitin films and fibers. *Green Chemistry, 12*(6), 968-971.

Ramesh, S., Liew, C.-W., & Arof, A. K. (2011a). Ion conducting corn starch biopolymer electrolytes doped with ionic liquid 1-butyl-3-methylimidazolium hexafluorophosphate. *Journal of Non-Crystalline Solids, 357*(21), 3654-3660.

Ramesh, S., Shanti, R., Morris, E., & Durairaj, R. (2011b). Utilisation of corn starch in production of 'green' polymer electrolytes. *Materials Research Innovations, 15*(1), s8.

Ramesh, S., Shanti, R., & Morris, E. (2012). Studies on the thermal behavior of CS:LiTFSI:[Amim] Cl polymer electrolytes exerted by different [Amim] Cl content. *Solid State Sciences, 14*(1), 182-186.

Sankri, A., Arhaliass, A., Dez, I., Gaumont, A. C., Grohens, Y., Lourdin, D., et al. (2010). Thermoplastic starch plasticized by an ionic liquid. *Carbohydrate Polymers, 82*(2), 256-263.

Schmitt, H., Guidez, A., Prashantha, K., Soulestin, J., Lacrampe, M. F., & Krawczak, P. (2015). Studies on the effect of storage time and plasticizers on the structural variations in thermoplastic starch. *Carbohydrate Polymers, 115*(0), 364-372.

Shi, R., Liu, Q., Ding, T., Han, Y., Zhang, L., Chen, D., et al. (2007). Ageing of soft thermoplastic starch with high glycerol content. *Journal of Applied Polymer Science, 103*(1), 574-586.

Tan, I., Flanagan, B. M., Halley, P. J., Whittaker, A. K., & Gidley, M. J. (2007). A method for estimating the nature and relative proportions of amorphous, single, and double-helical components in starch granules by ^{13}C CP/MAS NMR. *Biomacromolecules, 8*(3), 885-891.

van Soest, J. J. G., Hulleman, S. H. D., de Wit, D., & Vliegenthart, J. F. G. (1996). Crystallinity in starch bioplastics. *Industrial Crops and Products, 5*(1), 11-22.

van Soest, J. J. G., & Borger, D. B. (1997). Structure and properties of compression-molded thermoplastic starch materials from normal and high-amylose maize starches. *Journal of Applied Polymer Science, 64*(4), 631-644.

Vermeylen, R., Derycke, V., Delcour, J. A., Goderis, B., Reynaers, H., & Koch, M. H. J. (2006). Gelatinization of starch in excess water: Beyond the melting of lamellar crystallites. A combined wide- and small-angle x-ray scattering study. *Biomacromolecules, 7*(9), 2624-2630.

Wang, H., Gurau, G., & Rogers, R. D. (2012). Ionic liquid processing of cellulose. *Chemical Society Reviews, 41*(4), 1519-1537.

Wang, N., Zhang, X., Liu, H., & He, B. (2009a). 1-Allyl-3-methylimidazolium chloride plasticized-corn starch as solid biopolymer electrolytes. *Carbohydrate Polymers, 76*(3), 482-484.

Wang, N., Zhang, X., Wang, X., & Liu, H. (2009b). Communications: Ionic liquids modified montmorillonite/thermoplastic starch nanocomposites as ionic conducting biopolymer. *Macromolecular Research, 17*(5), 285-288.

Wang, N., Zhang, X., Liu, H., & Han, N. (2010). Ionically conducting polymers based on ionic liquid-plasticized starch containing lithium chloride. *Polymers & Polymer Composites, 18*(1), 53-58.

Wang, Q., Yang, Y., Chen, X., & Shao, Z. (2012). Investigation of rheological properties and conformation of silk fibroin in the solution of AmimCl. *Biomacromolecules, 13*(6), 1875-1881.

Wang, Q., Chen, Q., Yang, Y., & Shao, Z. (2013). Effect of various dissolution systems on the molecular weight of regenerated silk fibroin. *Biomacromolecules, 14*(1), 285-289.

Wendler, F., Todi, L.-N., & Meister, F. (2012). Thermostability of imidazolium ionic liquids as direct solvents for cellulose. *Thermochimica Acta, 528*(0), 76-84.

Wilhelm, H. M., Sierakowski, M. R., Souza, G. P., & Wypych, F. (2003). Starch films reinforced with mineral clay. *Carbohydrate Polymers, 52*(2), 101-110.

Wilpiszewska, K., & Spychaj, T. (2011). Ionic liquids: Media for starch dissolution, plasticization and modification. *Carbohydrate Polymers, 86*(2), 424-428.

768 Wu, Y., Sasaki, T., Irie, S., & Sakurai, K. (2008). A novel biomass-ionic liquid platform for the
769 utilization of native chitin. *Polymer, 49*(9), 2321-2327.
770 Xie, F., Halley, P. J., & Avérous, L. (2012). Rheology to understand and optimize processibility,
771 structures and properties of starch polymeric materials. *Progress in Polymer Science, 37*(4), 595-
772 623.
773 Xie, F., Pollet, E., Halley, P. J., & Avérous, L. (2013). Starch-based nano-biocomposites. *Progress in*
774 *Polymer Science, 38*(10-11), 1590-1628.
775 Xie, F., Flanagan, B. M., Li, M., Sangwan, P., Truss, R. W., Halley, P. J., et al. (2014). Characteristics
776 of starch-based films plasticised by glycerol and by the ionic liquid 1-ethyl-3-methylimidazolium
777 acetate: a comparative study. *Carbohydrate Polymers, 111*, 841-848.
778 Xie, F., Flanagan, B. M., Li, M., Truss, R. W., Halley, P. J., Gidley, M. J., et al. (2015). Characteristics
779 of starch-based films with different amylose contents plasticised by 1-ethyl-3-methylimidazolium
780 acetate. *Carbohydrate Polymers, 122*, 160-168.
781 Xie, H., Li, S., & Zhang, S. (2005). Ionic liquids as novel solvents for the dissolution and blending of
782 wool keratin fibers. *Green Chemistry, 7*(8), 606-608.
783 Xie, H., Zhang, S., & Li, S. (2006). Chitin and chitosan dissolved in ionic liquids as reversible sorbents
784 of CO_2. *Green Chemistry, 8*(7), 630-633.
785 Zakrzewska, M. E., Bogel-Łukasik, E., & Bogel-Łukasik, R. (2010). Solubility of carbohydrates in ionic
786 liquids. *Energy & Fuels, 24*(2), 737-745.
787 Zhang, B., Li, X., Liu, J., Xie, F., & Chen, L. (2013). Supramolecular structure of A- and B-type
788 granules of wheat starch. *Food Hydrocolloids, 31*(1), 68-73.
789 Zhang, B., Zhao, Y., Li, X., Li, L., Xie, F., & Chen, L. (2014). Supramolecular structural changes of
790 waxy and high-amylose cornstarches heated in abundant water. *Food Hydrocolloids, 35*, 700-709.

Zhang, B., Chen, L., Li, X., Li, L., & Zhang, H. (2015a). Understanding the multi-scale structure and functional properties of starch modulated by glow-plasma: A structure-functionality relationship. *Food Hydrocolloids, 50*, 228-236.

Zhang, B., Chen, L., Xie, F., Li, X., Truss, R. W., Halley, P. J., et al. (2015b). Understanding the structural disorganization of starch in water-ionic liquid solutions. *Physical Chemistry Chemical Physics, 17*(21), 13860-13871.

Zhang, H., Wu, J., Zhang, J., & He, J. (2005). 1-Allyl-3-methylimidazolium chloride room temperature ionic liquid: A new and powerful nonderivatizing solvent for cellulose. *Macromolecules, 38*(20), 8272-8277.

Zhu, S., Wu, Y., Chen, Q., Yu, Z., Wang, C., Jin, S., et al. (2006). Dissolution of cellulose with ionic liquids and its application: A mini-review. *Green Chemistry, 8*(4), 325-327.

Figure captions

Fig. 1 Moisture uptake results of the different starch-based films after ageing at 33% (L) or 75% (H) relative humidity.

Fig. 2 Tensile strength (σt) (a), Young's modulus (E) (b), and elongation at break (εb) (c) of the different starch-based films either before ageing, or after ageing at 33% (L) or 75% (H) relative humidity.

Fig. 3 TGA curves of pure [Emim][OAc], 9:1 (wt/wt) [Emim][OAc]:water solution, 3:7 (wt/wt) [Emim][OAc]:water solution, pure glycerol, 9:1 (wt/wt) glycerol:water solution, 3:7 (wt/wt) glycerol:water solution (a); native Gelose 80 starch, and the different starch-based films before ageing (b); and these films after ageing at either low (33%) and high (75%) relative humidity (c).

Fig. 4 XRD results of native G80 starch, and the different starch-based films either before ageing, or after ageing at 33% (L) and 75% (H) relative humidity.

Fig. 5 Synchrotron SAXS results (a), and their Lorentz-corrected patterns (b), for native G80 starch and different starch-based films before ageing.

Fig. 6 Lorentz corrected synchrotron SAXS results of the different starch-based films either before ageing, or after ageing at 33% (L) and 75% (H) relative humidity.

Fig. 7 FT-IR spectra of native G80 starch (a and b), [Emim][OAc] (a, b, and c), glycerol (a, b, and c) and different starch-based films before ageing (a, b), or after ageing (c) at 33% (L) and 75% (H) relative humidity.

Fig. 8 Raman spectra of native G80 starch, [Emim][OAc], glycerol, and different starch-based films either before ageing, or after ageing at 33% (L) and 75% (H) relative humidity.

Tables

Table 1 Samples codes, composition, and relative humidity during ageing, of the different starch-based films.

Code	Composition [a]				Storage
	Starch content [b]	Glycerol content	[Emim][OAc] content	Moisture content	Relative humidity (%)
S91/E9 [c]	90.52	–	9.48	0	–
S91/E9-L [d]	90.52	–	9.48	1.27±0.17	33
S91/E9-H [d]	90.52	–	9.48	8.13±0.18	75
S91/G9 [c]	90.52	9.48	–	0	–
S91/G9-L [d]	90.52	9.48	–	1.62±0.24	33
S91/G9-H [d]	90.52	9.48	–	8.78±0.67	75
S76/E24 [c]	76.09	–	23.91	0	–
S76/E24-L [d]	76.09	–	23.91	2.58±0.19	33
S76/E24-H [d]	76.09	–	23.91	17.74±1.06	75
S76/G24 [c]	76.09	23.91	–	0	–
S76/G24-L [d]	76.09	23.91	–	2.37±0.26	33
S76/G24-H [d]	76.09	23.91	–	14.47±0.48	75

[a] Portions in weight; [b] Dry weight; [c] films before ageing (0 days); [d] films aged for 42 days.

830 Table 2 XRD results of the different starch-based films

	XRD (%) [a]		
	Double helix (B-type)	Single helix (V-type)	Amorphous
Native G80	24.1	2.8	73.1
S91/E9	15.9	5.1	79.0
S91/E9-L	16.7	4.6	78.7
S91/E9-H	16.7	5.0	78.3
S76/E24	19.2	1.7	79.1
S76/E24-L	18.4	2.0	79.6
S76/E24-H	18.2	2.3	79.5
S91/G9	21.9	4.9	73.2
S91/G9-L	21.5	5.4	73.1
S91/G9-H	21.0	5.3	73.7
S76/G24	20.0	5.6	74.5
S76/G24-L	19.1	4.9	75.9
S76/G24-H	19.0	4.8	76.2

831 [a] XRD values are within ±2%.